Binding of C5-Dicarboxylic Substrate to Aspartate Aminotransferase: Implications for the Conformational Change at the Transaldimination Step † , ‡

6 AUTHORS, INCLUDING:

Hideyuki Hayashi
Osaka Medical College

120 PUBLICATIONS **3,212** CITATIONS

Binding of C5-Dicarboxylic Substrate to Aspartate Aminotransferase: Implications for the Conformational Change at the Transaldimination Step[†,‡]
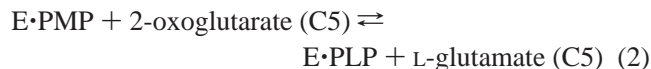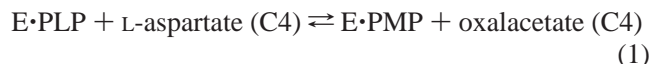
Mohammad Mainul Islam,[§,‖] Masaru Goto,[⊥] Ikuko Miyahara,[⊥] Hiroko Ikushiro,[§] Ken Hirotsu,[⊥] and Hideyuki Hayashi*,[§]

Department of Biochemistry, Osaka Medical College, 2-7 Daigakumachi, Takatsuki 569-8686, Japan, and Department of Chemistry, Graduate School of Science, Osaka City University, Osaka 558-8585, Japan

Received January 13, 2005; Revised Manuscript Received April 14, 2005

ABSTRACT: The mechanism for the reaction of aspartate aminotransferase with the C4 substrate, L-aspartate, has been well established. The binding of the C4 substrate induces conformational change in the enzyme from the open to the closed form, and the entire reaction proceeds in the closed form of the enzyme. On the contrary, little is known about the reaction with the C5 substrate, L-glutamate. In this study, we analyzed the pH-dependent binding of 2-methyl-L-glutamate to the enzyme and showed that the interaction between the amino group of 2-methyl-L-glutamate and the pyridoxal 5′-phosphate aldimine is weak compared to that between 2-methyl-L-aspartate and the aldimine. The structures of the Michaelis complexes of the enzyme with L-aspartate and L-glutamate were modeled on the basis of the maleate and glutarate complex structures of the enzyme. The result showed that L-glutamate binds to the open form of the enzyme in an extended conformation, and its α-amino group points in the opposite direction of the aldimine, while that of L-aspartate is close to the aldimine. These models explain the observations for 2-methyl-L-glutamate and 2-methyl-L-aspartate. The crystal structures of the complexes of aspartate aminotransferase with phosphopyridoxyl derivatives of L-glutamate, D-glutamate, and 2-methyl-L-glutamate were solved as the models for the external aldimine and ketimine complexes of L-glutamate. All the structures were in the closed form, and the two carboxylate groups and the arginine residues binding them are superimposable on the external aldimine complex with 2-methyl-L-aspartate. Taking these facts altogether, it was strongly suggested that the binding of L-glutamate to aspartate aminotransferase to form the Michaelis complex does not induce a conformational change in the enzyme, and that the conformational change to the closed form occurs during the transaldimination step. The hydrophobic residues of the entrance of the active site, including Tyr70, are considered to be important for promoting the transaldimination process and hence the recognition of the C5 substrate.

Aspartate aminotransferase (aspartate:2-oxoglutarate aminotransferase, EC 2.6.1.1; AspAT[1]) is one of the most extensively studied pyridoxal 5′-phosphate (PLP)-dependent enzymes. AspAT catalyzes the following ping pong Bi Bi reaction, where E·PLP and E·PMP denote the complex of the enzyme with PLP and the pyridoxamine 5′-phosphate (PMP), respectively.

$$\text{E·PLP} + \text{L-aspartate (C4)} \rightleftharpoons \text{E·PMP} + \text{oxalacetate (C4)} \tag{1}$$

$$\text{E·PMP} + \text{2-oxoglutarate (C5)} \rightleftharpoons \text{E·PLP} + \text{L-glutamate (C5)} \tag{2}$$

The overall reaction is a reversible transfer of the α-amino group between aspartate and 2-oxoglutarate and is composed of two half-reactions in which the α-amino group temporarily resides on the coenzyme PLP to form PMP (*1*). Thus, AspAT is active toward two types of dicarboxylic acids different in chain length. Aspartate and the corresponding keto acid oxalacetate are called C4 substrates and glutamate and the 2-oxoglutarate C5 substrates.

Combined spectroscopic, kinetic, and structural studies have elucidated the course of the catalytic reaction of AspAT with C4 substrates (Scheme 1; *2−10*). The aldehyde group of PLP is covalently linked to the ε-amino group of Lys258[2]

[1] Abbreviations: AspAT, aspartate amino acid aminotransferase (aspartate:2-oxoglutarate aminotransferase, EC 2.6.1.1); HEPES, 1-(2-hydroxyethyl)piperazine-4-(2-ethanesulfonic acid); L-MeAsp, 2-methyl-L-aspartate; L-MeGlu, 2-methyl-L-glutamate; MES, 4-morpholineethanesulfonic acid; PIPES, 1,4-piperazine-bis(ethanesulfonic acid); TAPS, 3-((tris(hydroxymethyl)methyl)amino)-1-propanesulfonic acid; PLP, pyridoxal 5′-phosphate; PMP, pyridoxamine 5′-phosphate; PPx, phosphopyridoxyl; RMSD, residual mean square deviation.

[2] The amino acid residue numbers are those of pig cytosolic aspartate aminotransferase (*11*). The 16 residues of the pig cytosolic enzyme (412 residues) which has no corresponding residues in the *E. coli* enzyme (396 residues) are Ala1, Pro2, Pro3, Ser4, Ser65, Asn127, Asn128, Asp130, Thr131, Pro132, Lys153, Asn232, Ala407, Lys410, Ile411, and Gln412. The asterisk (e.g., Tyr70*) indicates that the residue comes from the other subunit of the dimer molecule.

Scheme 1: Reaction Mechanism of Aspartate Aminotransferase with L-Aspartate
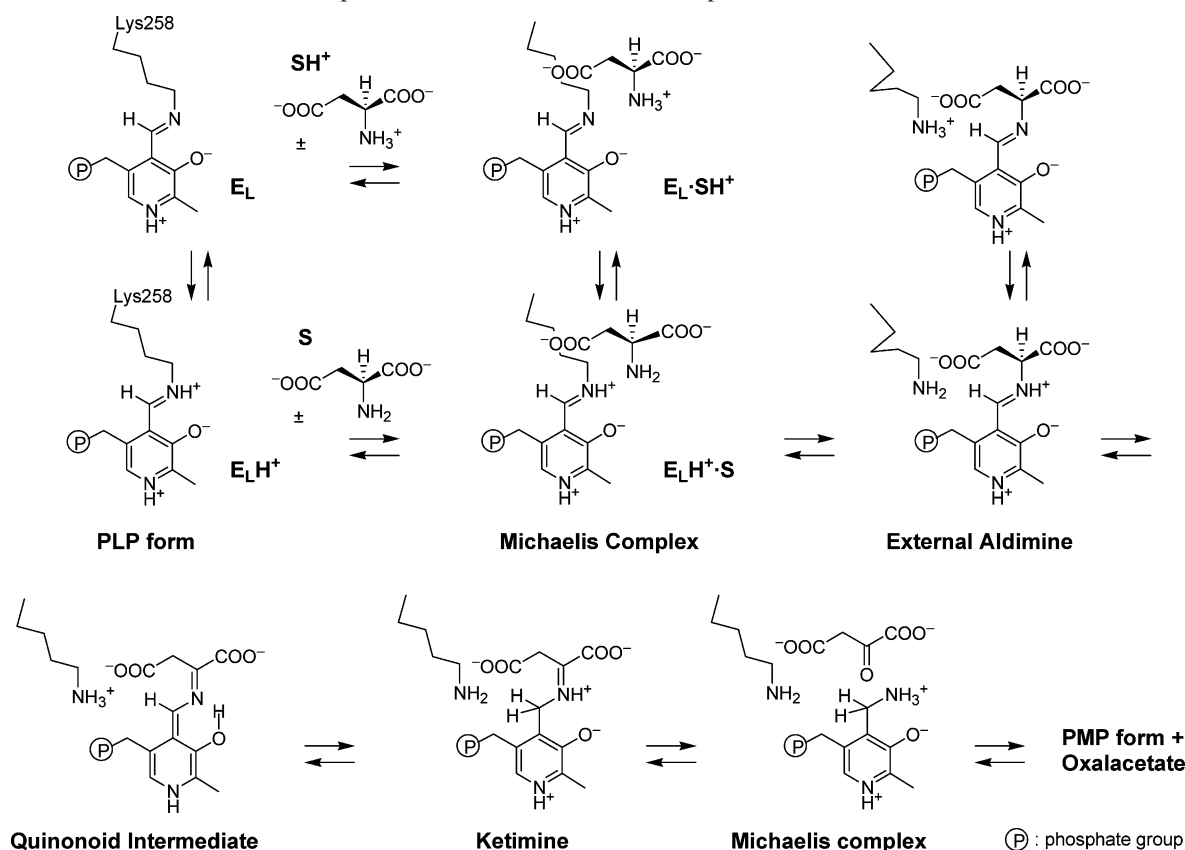
at the active site of the enzyme (internal aldimine). The pK_a of the PLP−Lys258 Schiff base is low compared to the usual PLP Schiff bases in aqueous solutions, and at neutral pH E·PLP exists as an equilibrium mixture of the Schiff-base-protonated form (E_LH^+) and the unprotonated form (E_L). The α-amino-group-protonated form of aspartate (SH^+) binds to E_L, and the unprotonated form (S) binds to E_LH^+. Thus, the Michaelis complex is a rapid-equilibrium mixture of the two species, $E_L \cdot SH^+$ and $E_LH^+ \cdot S$. The species $E_LH^+ \cdot S$ undergoes a transaldimination reaction to form a species in which a Schiff base between PLP and aspartate is formed (the external aldimine complex). The external aldimine is converted to its tautomer, ketimine, by a 1,3-prototropic shift catalyzed by the liberated ε-amino group of Lys258. After hydrolysis, the Michaelis complex of oxalacetate and E·PMP are formed. Dissociation of this complex yields E·PMP and oxalacetate.

The AspAT protein is a dimer of identical subunits, each composed of large and small domains. The molecule has two active site pockets around the molecular 2-fold axis. Each pocket is located at the domain interface of one subunit and at the subunit interface. The complexes of E·PLP with maleate (*3*, *4*) and 2-methyl-L-aspartate (*5*, *6*), and the complex of E·PMP with maleate (*7*) are the models for the Michaelis complex with aspartate, the external aldimine, and the Michaelis complex with oxalacetate, respectively. All of these complexes show the closed form of the overall structure, in which the small domain approaches the large domain and closes the active site. That is, the catalytic reaction of AspAT with the C4 substrate described above is carried out in the closed structure of the enzyme. The electrostatic and hydrophobic interactions between the active

site residues and the substrate are responsible for maintaining the closed structure (*2*).

The C5-dicarboxylic substrates have the same terminal functional groups as the C4-dicarboxylic substrates. With this structural similarity, it can be considered that the reaction of the C5 substrates (eq 2) is carried out essentially in the same way as that of the C4 substrates (eq 1). The dissociation constant values for C5-dicarboxylic ligands, however, are generally over 10 times those of the corresponding C4-dicarboxylic ligands. Due to the expected difficulty in analyzing the spectroscopic changes induced by the C5-dicarboxylic ligands, little is known about the reactions with C5 substrates compared to those of C4 substrates.

Recently, we have shown by kinetic analysis that the Michaelis complex with glutamate has more protonation states than the complex with aspartate (*12*), the latter of which has exclusively one proton on its imino and amino groups (*10*). This indicates that, albeit the outline of the catalytic cycle should be essentially the same, there are distinct differences in the detailed mechanism between the C5 substrate−AspAT and the C4 substrate−AspAT reactions. In this study, we investigated further spectroscopically and structurally the complex of AspAT with C5 ligands and proposed that AspAT undergoes a conformational change during the conversion from the Michaelis complex to the external aldimine on reaction with L-glutamate.

EXPERIMENTAL PROCEDURES

Chemicals. Escherichia coli AspAT was obtained as described earlier (*13*) using *E. coli* JM103 containing pUC19−*aspC*. 2-Methyl-DL-glutamic acid was purchased

from Sigma. Buffer components used are MES, PIPES, HEPES, and TAPS.

Preparation of 2-Methyl-L-glutamic Acid. The L form of 2-methylglutamic acid was separated from 5 g of the racemic mixture as follows. A 0.1 mL solution of 100 mM 2-methyl-DL-glutamic acid was injected into a preparative (10 × 250 mm) reversed-phase HPLC column (Cosmosil 5C18M-II, Nakarai Chemicals, Kyoto, Japan) equilibrated with 40 mM $CuSO_4$ and 80 mM L-proline, pH 5.5 adjusted with 6 M HCl, on a Beckman HPLC system (System Gold; model 126 solvent module and model 168 detector). The flow rate of the mobile phase was fixed at 4 mL min^{-1} with a pressure of around 17 MPa, and the eluent was monitored by measuring the absorbance at 580 nm (corresponding to an equimolar chelate complex between Cu^{2+}, L-proline, and 2-methylglutamate). The D and L forms were eluted at 4.2 and 6.0 min, respectively. The chromatography was repeated, and the fraction containing 2-methyl-L-glutamic acid was pooled and concentrated 10 times in a rotary evaporator. The solution was then applied to a Dowex 50 × 8 cation exchange column (25 × 200 mm, H$^+$ form), which had been activated with 2 M formic acid and washed briefly with H_2O. The sample was eluted by 0.2 M formic acid. The fraction containing 2-methyl-L-glutamic acid was detected by ninhydrin. The collected 2-methyl-L-glutamic acid was concentrated and crystallized in 70% ethanol. The yield was about 80% (starting from the L form).

Synthesis of Phosphopyridoxyl-glutamate and Phosphopyridoxyl-2-methylglutamate. Two millimoles of PLP was mixed with 10 mmol of L-glutamic acid in 20 mL of water, and the pH was adjusted to 9.4 with KOH. With stirring, 0.2 g of $NaBH_4$ was then added slowly to reduce the Schiff base. The reaction mixture was incubated for 10 min. Twenty milliliters of 0.2 M formic acid was added, and the solution was applied to a Dowex 1 × 8 anion-exchange resin column (10 × 160 mm) equilibrated with 0.1 M formic acid. The column was washed with 120 mL of 0.1 M formic acid and eluted with a linear gradient formed with 100 mL each of 0.1 and 0.3 M formic acid. Fractions were spotted onto a filter paper, and substances were detected first with fluorescence (excited at 214 nm) and then with ninhydrin. A trace amount of pyridoxine 5′-phosphate (fluorescence (+), ninhydrin (−)) is eluted first, followed by the unreacted glutamic acid (fluorescence (−), ninhydrin (+)), then *N*-phosphopyridoxyl-L-glutamic acid (fluorescence (+), ninhydrin (−)). Fractions containing *N*-phosphopyridoxyl-L-glutamic acid were collected and rotary evaporated to give an oily residue. Three milliliters of 6 M HCl was added and rotary evaporated. The residue was dissolved in 3 mL of H_2O, and 6 mL of EtOH and 12 mL of Et$_2$O were then added to the solution and left at 4 °C overnight. The viscous oily layer is the phosphopyridoxyl-L-glutamic acid. The phosphopyridoxyl derivative of D-glutamic acid and 2-methyl-L-glutamic acid was prepared in the same way.

Construction of AspAT Complexed with either Phosphopyridoxyl-glutamate or Phosphopyridoxyl-2-methylglutamate. The apo form of AspAT was prepared according to the method of Toney and Kirsch (9). The enzyme was reconstituted with a 10-fold excess of phosphopyridoxyl-L-glutamate (PPx-L-Glu), phosphopyridoxyl-D-glutamate (PPx-D-Glu), or phosphopyridoxyl-2-methyl-L-glutamate (PPx-L-MeGlu). The mixture was incubated at room temperature

Table 1: Data Collection for Refinement Statistics

crystal	L-glutamate	methyl-L-glutamate	D-glutamate
space group	$P6_3$	$P6_3$	$P6_3$
a, b (Å)	143.83	143.21	142.71
c (Å)	81.57	81.39	81.39
diffraction data			
resolution (Å)	2.4	2.2	2.2
no. of reflns			
unique	36675	47797	42792
observed	125959	155510	81915
completeness (%)	97.3 (99.6)^a	98.9 (99.8)^a	89.1 (82.0)^a
R_{merge} (%)^b	10.4 (29.8)^a	7.7 (25.1)^a	6.4 (27.8)^a
refinement			
resolution limits (Å)	49.4−2.4	49.4−2.2	49.4−2.2
R_{factor} (%)^c	19.8 (24.8)^a	19.5 (24.8)^a	19.3 (25.2)^a
R_{free} (%)^d	24.2 (29.5)^a	23.2 (28.4)^a	23.5 (29.3)^a
deviations			
bond lengths (Å)	0.007	0.006	0.007
bond angles (deg)	1.31	1.26	1.28
mean B factors			
main-chain atoms (Å^2)	30.92	33.32	29.20
side-chain atoms (Å^2)	32.92	35.94	31.31
heteroatoms (Å^2)	27.79	29.86	22.86
water atoms (Å^2)	32.89	39.27	36.95
procheck			
favored	89.3	91.8	90.1
additional allowed	10.5	7.9	9.5
generously allowed	0.0	0.0	0.1
disallowed	0.3	0.3	0.3

^{a} The values in parentheses are for the highest resolution shells. ^{b} $R_{merge} = \sum_{hkl}\sum_i |I_{hkl} - \langle I_{hkl} \rangle| / \sum_{hkl}\sum_i I_{hkl}$ where I is the observed intensity and $\langle I \rangle$ is the average intensity for multiple measurements. ^{c} $R_{factor} = \sum ||F_o| - |F_c|| / |F_o|$. ^{d} R_{free} was monitored with 10% of the reflection data excluded from the refinement.

for 30 min and passed through a PD-10 column (Amersham) equilibrated with 10 mM Tris-HCl, pH 7.5, to remove the excess ligand. The obtained enzyme solution was used for crystallization. The reconstituted enzymes are denoted as E·PPx-L-Glu, E·PPx-D-Glu, and E·PPx-L-MeGlu, respectively.

Preparation of Crystals. The crystals of AspATs reconstituted with PPx-L-Glu, PPx-D-Glu, and PPx-L-MeGlu were obtained by the hanging drop vapor diffusion method (14) using ammonium sulfate as the precipitant. A 3 μL drop containing 30 mg mL^{-1} enzyme, 10 mM Tris-HCl (pH 7.5), 10 μM PLP, 1 mM EDTA, and 0.3 mM NaN$_3$ was added to 3 μL of the precipitant buffer containing 2 M ammonium sulfate, 100 mM HEPES (pH 7.5), and 4% (w/v) PEG-400 and equilibrated with a reservoir solution containing 2 M ammonium sulfate, 100 mM HEPES (pH 7.5), and 4% (w/v) PEG-400 at 293 K. The crystallization conditions are exactly the same as those in the previous studies of the PLP form (6) and the PMP form (7) of *E. coli* AspAT. Crystals of suitable size for diffraction experiments were obtained within a week.

Data Collection. The space group is $P6_3$ having averaged cell dimensions of $a = b = 143.25$ Å and $c = 81.45$ Å. Crystals of AspATs contain two subunits in the asymmetric unit with about 48% of the crystal volume occupied by solvent.

The X-ray diffraction data for the AspAT crystals were collected to 2.2 Å resolutions at 293 K with a Rigaku R-AXIS IV^{++}. The intensity data were processed and scaled using HKL2000/SCALEPACK. The conditions for data collection are summarized in Table 1.

Structure Determination and Refinement. The structures of AspATs were solved by the molecular replacement method, using the complex of the PMP form of AspAT with glutarate (*7*; PDB ID: 1AMS) as an initial search model. The scaling of all data and map calculations was performed with the CCP4 program suite (*15*). The initial model of AspAT was built with the program O (*16*). The model was refined with the simulated annealing, individual *B* factor refinement, and energy minimization protocols incorporated into the program CNS (*17*). After the initial round of refinement, the model was refined against the highest resolution data. When the R_{factor} value reached below 30%, $2F_o - F_c$ simulated annealing omit maps contoured at 1.0σ clearly exhibited the residual electron density corresponding to the bound sulfates. Water molecules were picked up from the $F_o - F_c$ map on the basis of reasonable hydrogen-bonding geometries and significant densities at 2.0σ.

The final model of E·PPx-L-Glu consisted of 396×2 residues, 129 water molecules, and one PPx-L-MeGlu with an R_{factor} of 19.8% at a 2.4 Å resolution. Alanine models were applied to 24 residues (Arg25, Lys90, Lys121, Lys126, Lys367, Leu371, Arg25*, Lys46*, Glu78*, Arg81*, Lys90*, Lys98*, Lys126*, Arg129*, Glu164*, Asn178*, Gln181*, Gln210*, Glu214*, Lys248*, Gln342*, Arg348*, Lys355*, and Lys367*; the asterisk indicates a residue from another subunit of the dimer unit), because the electron densities corresponding to the side chains of these residues were weak or not observed.

The final model of E·PPx-D-Glu consisted of 396×2 residues, 204 water molecules, and one PPx-D-MeGlu with an R_{factor} of 19.3% at a 2.2 Å resolution. Alanine models were applied to 29 residues (Arg25, Lys90, Lys121, Lys126, Gln210, Glu343, Lys367, Arg25*, Glu43*, Lys46*, Glu78*, Arg81*, Lys90*, Lys98*, Lys126*, Glu164*, Asn175*, Asn178*, Glu179*, Gln181*, Gln210*, Glu214*, Lys215*, Lys248*, Asn347*, Arg348*, Lys355*, Lys367*, and Glu368*).

The final model of E·PPx-L-MeGlu consisted of 396×2 residues, 191 water molecules, and one PPx-L-MeGlu with an R_{factor} of 19.5% at a 2.2 Å resolution. Alanine models were applied to 21 residues (Arg25, Glu28, Lys46, Lys90, Lys121, Lys126, Gln206, Lys367, Glu368, Arg25*, Arg81*, Lys90*, Lys98*, Lys126*, Glu164*, Gln210*, Glu214*, Lys215*, Lys248*, Lys355*, and Lys367*).

A summary of the refinement statistics for all structures is presented in Table 1. The quality of the final structures was assessed using the program PROCHECK (*18*). For all structures, Ser296 and Ser296* were found in disallowed regions of the Ramachandran plot. On the basis of the electron density map, it is confirmed that the conformations of both residues are correct.

Modeling of the Michaelis Complex Structures of AspAT with L-Glutamate and L-Aspartate. For the Michaelis complex of E·PLP with L-glutamate (E·PLP·L-glutamate), the crystal structure of the PMP form of *E. coli* AspAT with glutarate (*7*; 1AMS) was used for modeling. PMP and glutarate were changed to PLP and L-glutamate, respectively, and the aldehyde group of PLP was bonded to the ε-amino group of Lys258. Energy minimization was carried out on MOE (ver. 2004.03, Chemical Computing Group Inc., Montréal, Canada) using MMFF94s parameters with all the residues fixed except for those interacting with the PLP—Lys258 aldimine and

L-glutamate: Asp222, Trp140, Arg266, Tyr225, Asn194, Tyr70*, Arg292*, Ser296*, Arg386, Leu17, Ile18, Ile37, Gly38, and Val39. The hydrogen atoms of crystal water molecules were allowed to move. The N atoms of the PLP—Lys258 aldimine and pyridine were protonated, and O3′ of PLP was unprotonated. The charge of the phosphate group was set at -2, as has been demonstrated by ^{31}P NMR (*19*). The α-amino group of L-glutamate was either protonated or unprotonated. The protonation status of the α-amino group affected the energy-minimized structure of L-glutamate. For the Michaelis complex of E·PLP with L-aspartate (E·PLP·L-aspartate), the crystal structure of *E. coli* AspAT complexed with maleate (*4*; 1ASM) was used for modeling. Maleate was changed to L-aspartate with an unprotonated α-amino group, and energy minimization was carried out in the same way as above.

For studying the differential effect of L-glutamate and L-aspartate on the open—closed conformation of the Michaelis complex of AspAT, the model study was conducted as follows. Either L-aspartate or L-glutamate was modeled into the active site of the closed form of the enzyme, and energy minimization was carried out as above, but in this case all the atoms were allowed to move. For the complex with L-aspartate, the obtained model of E·PLP·L-aspartate described above was used as the starting structure. For the complex with L-glutamate, the structure of E·PPx-L-MeGlu was used as the template. The L-MeGlu moiety was changed to L-glutamate while the dihedral angles and position of the carbon skeleton were maintained. The α-amino group of L-glutamate was protonated. The phosphopyridoxyl group and Lys258 were removed, and the PLP—Lys258 Schiff base was incorporated from the crystal structure of E·PLP (*6*; 1ARS). Crystal water molecules were included in the model with the exceptions of WAT2017 (subunit 1) and WAT2014 (subunit 2), which are hydrogen bonded to Ser296* and are expected to interfere with the binding of the substrate γ-carboxylate group to this region. After energy minimization, an almost symmetric dimeric structure, in which L-glutamate assumes a similar conformation in both subunit 1 and subunit 2, was obtained. Then, a stochastic conformational search (implemented in MOE) was performed on L-glutamate in subunit 1, and another energetically favorable structure of E·PLP·L-glutamate with a more extended conformation of L-glutamate was obtained.

Graphics. Superimposition of the structures and the molecular drawings were performed using MOLMOL (*20*; Figures 3 and 5) and PyMOL (*21*; Figures 4 and 6).

RESULTS

pH Titration of the Complex of E·PLP with 2-methyl-L-glutamate. The spectral changes of the PLP form of AspAT (E·PLP) on binding of 2-methyl-L-glutamate (L-MeGlu) were studied at various pH values between 6 and 9. At all pH values studied, the binding of L-MeGlu to E·PLP caused an increase in the absorption at 430 nm with a concomitant decrease in the absorption at 360 nm (Figure 1).

The spectrum of the complex of E·PLP with L-MeGlu at each pH value was obtained by extrapolation to infinite concentrations of L-MeGlu, and the absorption at 430 nm was plotted against the pH of the solution (Figure 2). Due to the near linear dependency on the L-MeGlu concentration
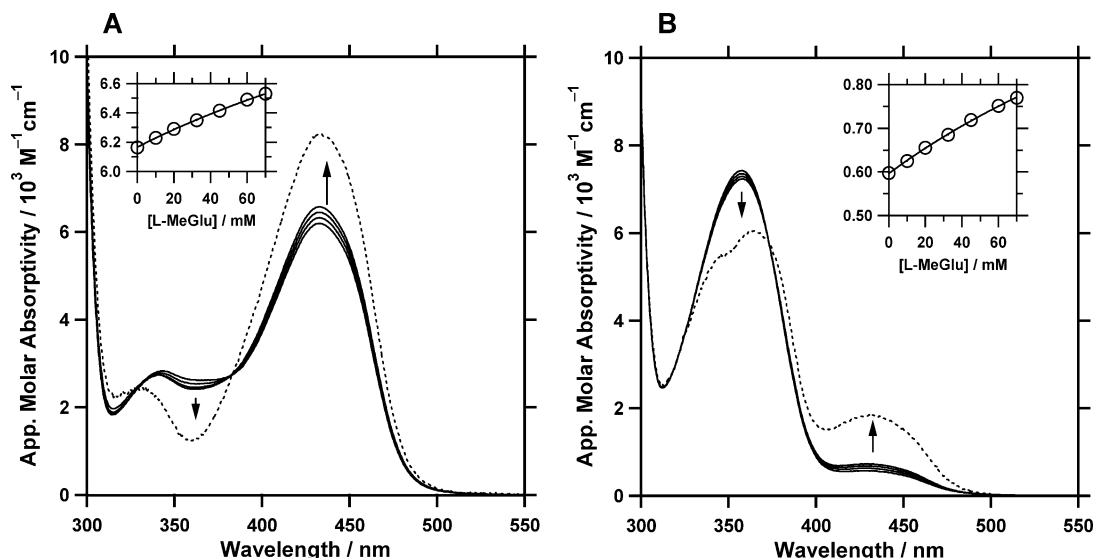
FIGURE 1: Spectral change in AspAT on binding of L-MeGlu. Absorption spectra were measured in the presence of 50 mM buffer component(s), 0.1 M KCl, and 0, 20, 45, and 70 mM L-MeGlu at 298 K. Results at pH 6.1 (A) and pH 7.1 (B) are shown. The insets show plots of the apparent molar absorptivity against [L-MeGlu]. The dashed lines show the spectrum at infinite concentrations of L-MeGlu obtained by extrapolation using $\epsilon_{app} = \{[L\text{-MeGlu}]/(K_d + [L\text{-MeGlu}])\}\epsilon_{max}$.
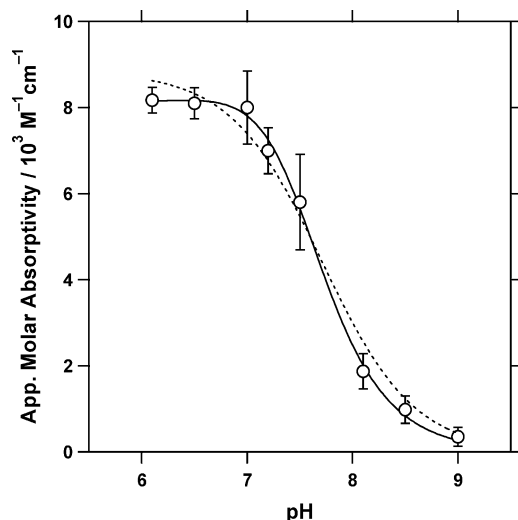

FIGURE 2: Plot of the apparent molar absorptivity at 430 nm of the complex of E·PLP with L-MeGlu (ϵ_{max} in Figure 1) against pH. The bars indicate SD values. The solid line shows the theoretical line using eq 3, with $\alpha = 1.19 \pm 0.31$, $pK_{a1} = 7.44 \pm 0.10$, $pK_{a2} = 7.50 \pm 0.33$, and $\epsilon = 8100 \pm 270$ $M^{-1}\cdot cm^{-1}$. The dashed line shows the theoretical line using a single-step dissociation model: $\epsilon_{app,max} = \{[H^+]/(K_a + [H^+])\}\epsilon$, with $pK_a = 7.71 \pm 0.08$ and $\epsilon = 8830 \pm 350$ $M^{-1}\cdot cm^{-1}$.

at pH values 7–8, the obtained apparent molar absorptivity values have large SD values. However, there is a clear tendency that the value declines sharply with increasing pH. The plots were simulated with the two-step dissociation model:

$$\epsilon_{app,max} = \frac{\alpha K_{a2}[H^+] + [H^+]^2}{K_{a1}K_{a2} + K_{a2}[H^+] + [H^+]^2}\epsilon \qquad (3)$$

Here K_{a1} and K_{a2} are the dissociation constants for the two consecutive dissociation processes (Scheme 2, $E_LH^+\cdot SH^+ \rightleftarrows (E_LH^+\cdot S + E_L\cdot SH^+) \rightleftarrows E_L\cdot S$, where $E_LH^+\cdot S$ and $E_L\cdot SH^+$ are treated as a single species), and ϵ and $\alpha\epsilon$ are the apparent molar absorptivity values of the doubly protonated species,

$E_LH^+\cdot SH^+$, and singly protonated species, $E_LH^+\cdot S$ plus $E_L\cdot SH^+$, respectively (Scheme 2). Excellent fitting was obtained with the following values of the parameters: $\alpha = 1.19 \pm 0.31$, $pK_{a1} = 7.44 \pm 0.10$, $pK_{a2} = 7.50 \pm 0.33$, and $\epsilon = 8100 \pm 270$ $M^{-1}\cdot cm^{-1}$. The value of α is expected to be roughly equal to the value of $[E_LH^+\cdot S]/([E_LH^+\cdot S] + [E_L\cdot SH^+])$; therefore, the obtained value of α indicates that the equilibrium between $E_LH^+\cdot S$ and $E_L\cdot SH^+$ is shifted toward $E_LH^+\cdot S$. In addition, the fitting was much better than that with a single-step dissociation model (dashed line), indicating that the term $[H^+]^2$ is required for the fitting. From this and the previous result of the kinetic characterization of the reaction of E·PLP with L-glutamate, we concluded that the Michaelis complex of E·PLP with L-MeGlu contains the four species $E_LH^+\cdot SH^+$, $E_LH^+\cdot S$, $E_L\cdot SH^+$, and $E_L\cdot S$ (Scheme 2). This is in contrast to the case of 2-methyl-L-aspartate (L-MeAsp), where the Michaelis complex of E·PLP with L-MeAsp shows pH-independent partial protonation of the aldimine (*22*), and the Michaelis complex contains only $E_LH^+\cdot S$ and $E_L\cdot SH^+$.

Models for the Michaelis Complexes of E·PLP with L-Aspartate and L-Glutamate. In order to structurally explain the electrostatic interaction of the dissociation groups in the Michaelis complexes of E·PLP with L-aspartate and L-glutamate, models were constructed based on the crystal structures of AspAT with substrate analogues.

The structure of the Michaelis complex of E·PLP with L-aspartate (E·PLP·L-Asp) was modeled on the maleate complex of E·PLP (*4*). The α- and β-carboxylate groups of L-aspartate form a double hydrogen bond with the guanidinium groups of Arg386 and Arg292*, respectively (Figure 3A), as has been suggested from a number of crystal structures of AspAT complexed with C4-dicarboxylic ligands. The α-amino group of L-aspartate is pointed toward the PLP aldimine, and the distance between the α-amino N and the aldimine N is 3.4 Å, indicating a strong electrostatic interaction between the two N atoms.

For the modeling of the Michaelis complex of E·PLP with L-glutamate, X-ray crystallographic structures of E·PLP

Scheme 2:   Scheme for the Reaction of Aspartate Aminotransferase with L-Glutamate
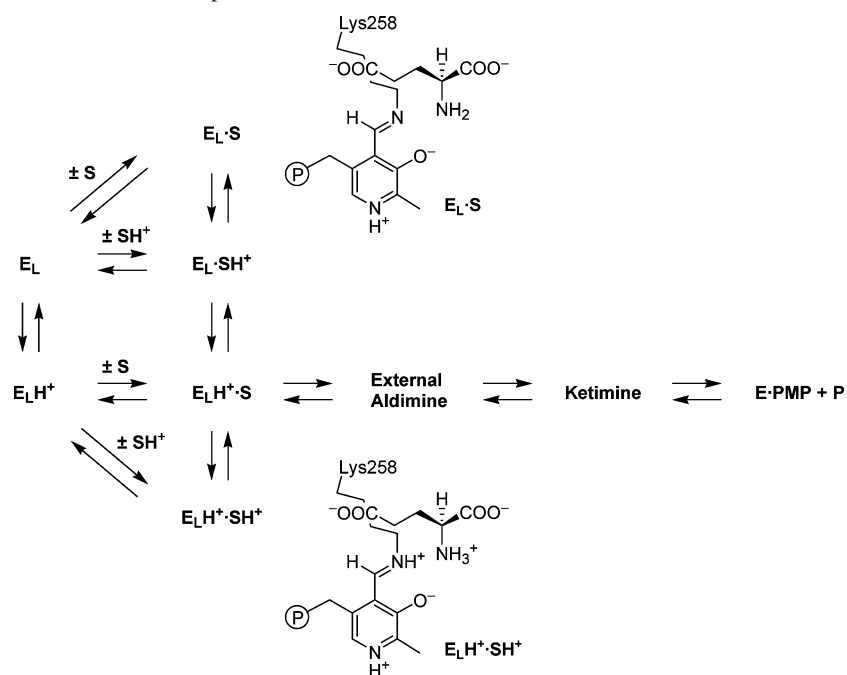
bound with C5-dicarboxylic ligands, such as L-MeGlu or glutarate, are required. However, attempts at cocrystallization of E·PLP with either L-MeGlu or glutarate have been unsuccessful. Instead, the crystal structure of E·PMP with glutarate has been obtained (*7*), and this is the only structure of the C5 complex of the wild-type AspAT obtained by cocrystallization. The structure showed that the AspAT protein is in the open conformation, and the glutarate molecule assumes an extended conformation at the active site. There is no apparent interaction between the carboxylate groups of glutarate and the amino group of PMP or the ε-amino group of Lys258, and the carboxylate groups are bound to Arg292*, Ser296*, and Arg386, which is a common structure between E·PLP and E·PMP. Furthermore, the
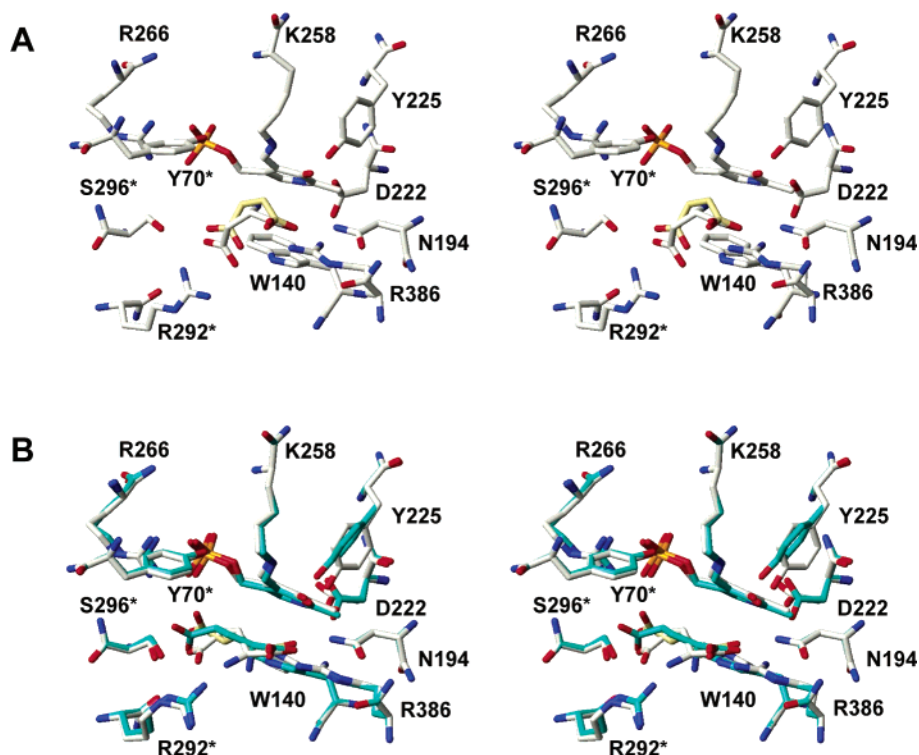

FIGURE 3: (A) Stereoview of the structure of the Michaelis complex of the E·PLP with L-aspartate modeled on the crystallographic structure of E·PLP with maleate (*4*; 1ASM). Nitrogen, oxygen, and phosphate atoms are colored in blue, red, and orange, respectively. (B) Stereoview of the structure of the Michaelis complex of E·PLP with L-glutamate modeled on the crystallographic structure of the complex of E·PMP with glutarate (*7*; 1AMS). Two structures, one with an unprotonated α-amino group of L-glutamate and the other with a protonated α-amino group, were generated and differentiated by coloring the carbon atoms in cyan (unprotonated α-amino group) and white (protonated α-amino group). Maleate (A) and glutarate (B) in the original coordinates are shown with carbon atoms in khaki. For the minimization procedure, see Experimental Procedures.
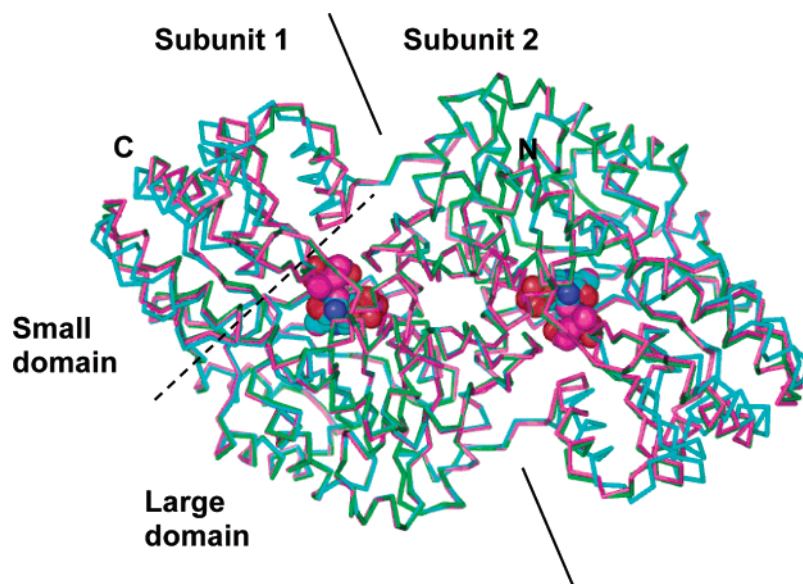
FIGURE 4: Superimposed Cα traces of the crystal structures of E·PLP (cyan), E·PLP=L-MeAsp (green), and E·PPx-L-MeGlu (magenta). The backbone atoms of the large domain (residues 43−325) of the dimeric structures were fitted. PLP of E·PLP and PPx-L-MeGlu of E·PPx-L-MeGlu are shown in van der Waals spheres. The enzyme is a dimer of identical subunits, each composed of large and small domains. The domain boundary of subunit 1 is shown by the dashed line. N and C indicate the N-terminus and C-terminus of subunit 1.

maleate (C4) complex of E·PMP assumes a closed conformation like that of the maleate complex of E·PLP. Therefore, we considered that the presence of PMP instead of PLP is not the cause of the obtained open conformation of the glutarate complex of E·PMP, and we used this structure for modeling the Michaelis complex of E·PLP with L-glutamate (E·PLP·L-Glu).

In E·PLP·L-Glu, the α-carboxylate group of L-glutamate forms a double hydrogen bond with the guanidinium group of Arg386 (Figure 3B), in a way similar to that of L-aspartate in E·PLP·L-Asp (Figure 3A). However, the structure of E·PLP·L-Glu (Figure 3B) is different from that of E·PLP·L-Asp on a number of points. When the α-amino group of L-glutamate is unprotonated (Figure 3B, carbon atoms in cyan), L-glutamate assumes an extended conformation like that of glutarate in the crystal structure (*7*). Like E·PLP·L-Asp, the side chain of Arg292* swings into the active site, and its guanidinium group interacts with the distal (γ-) carboxylate group of L-glutamate. However, the γ-carboxylate group forms a single hydrogen bond with the guanidinium group of Arg292*, i.e., only one of the O atoms interacts with the guanidinium N of Arg292*. In addition, the same O atom is within hydrogen-bond distance (2.5 Å) to the O atom of Ser296*. This additional hydrogen bond, which is absent in E·PLP·L-Asp (Figure 3A; the corresponding distance is 3.6 Å), seems to contribute to stabilizing the γ-carboxylate group of the extended structure. The α-amino group of L-glutamate is pointed in the direction opposite to the PLP−Lys258 aldimine and is within hydrogen-bond distance (2.8 Å) to the pyrrole N of Trp140, thereby stabilizing the bound L-glutamate. When the α-amino group of L-glutamate is protonated (Figure 3B; carbon atoms in white), the resultant structure is essentially similar to that of the L-glutamate with unprotonated α-amino group described above, except that the protonated α-amino group no longer forms a hydrogen bond with the pyrrole N of Trp140 and instead forms an intramolecular hydrogen bond/salt bridge with the γ-carboxylate group of L-glutamate. As a result,

L-glutamate assumes a somewhat round conformation compared to that of the L-glutamate with an unprotonated α-amino group.

Structure of AspAT Complexed with C5 Ligands. The X-ray diffraction data of AspATs reconstituted with PPx-L-Glu (E·PPx-L-Glu), PPx-D-Glu (E·PPx-D-Glu), and PPx-L-MeGlu (E·PPx-L-MeGlu) were collected at 2.4, 2.2, and 2.2 Å resolutions, respectively (Table 1).

The backbone structure of E·PPx-L-MeGlu is superimposed on that of E·PLP, together with the external aldimine complex of E·PLP with L-MeAsp (E·PLP=L-MeAsp) in Figure 4. The large domain main-chain atoms (residues 43−325 of each of the two subunits) of E·PPx-L-MeGlu are excellently fitted to those of E·PLP with an RMSD of 0.32 Å, which can be compared to the corresponding value of 0.28 Å between E·PLP=L-MeAsp and E·PLP. The small domain (residues 5−42 and 326−409) of E·PPx-L-MeGlu moves toward the large domain compared to that of E·PLP (Figure 4). The RMSD values of the small domain main-chain atoms between E·PLP and E·PPx-L-MeGlu are 1.83 Å (subunit 1) and 1.94 Å (subunit 2), comparable to the corresponding value (1.97 Å) between E·PLP=L-MeAsp and E·PLP. On the other hand, the RMSD values of the small domain main-chain atoms between E·PPx-L-MeGlu and E·PLP=L-MeAsp are 0.57 Å (subunit 1) and 0.63 Å (subunit 2). Especially, the backbone chains around the active site of the two structures are almost completely superimposed (Figure 4). Thus, E·PPx-L-MeGlu, which can be considered to be a model for the external aldimine complex of E·PLP with L-glutamate, assumes a closed conformation similar to that generated by the binding of L-MeAsp to E·PLP (*5, 6*).

The structures of E·PPx-L-Glu and E·PPx-D-Glu were essentially identical to that of E·PPx-L-MeGlu (data not shown for E·PPx-L-Glu; for E·PPx-D-Glu, see below).

Comparison of the Active-Site Structures of E·PPx-L-MeGlu and E·PLP=L-MeAsp. The active-site structure of E·PPx-L-MeGlu is shown in Figure 5A in comparison with
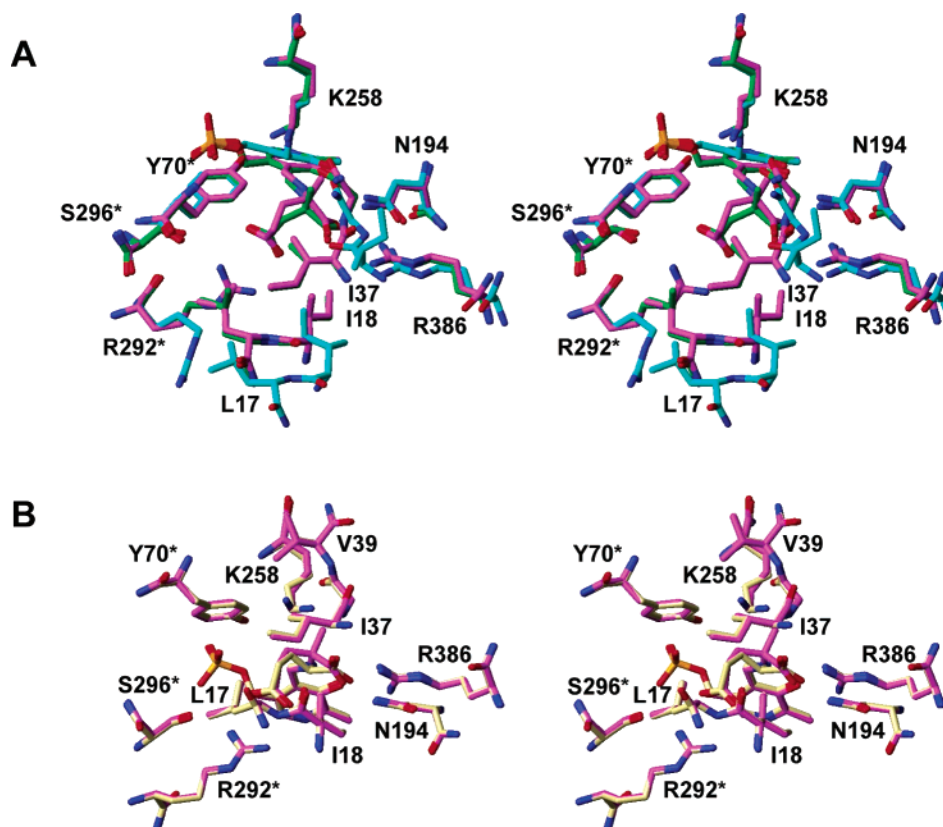
FIGURE 5: (A) Superimposed crystal structures of the active site of AspAT complexed with various ligands. N, O, and P atoms are shown in blue, red, and orange, respectively. Three structures are distinguished by the color of the carbon atoms: cyan, E·PLP (*6*: 1ARS); green, E·PLP=L-MeAsp (*6*; 1ART); magenta, E·PPx-L-MeGlu (this study). Structures were fitted to the main-chain atoms of the large domains. (B) Superimposed structures of the active site of E·PPx-L-MeGlu (carbon in magenta) and E·PPx-D-Glu (carbon in khaki). Structures were fitted to the main-chain atoms of the large domains. In both panels, residues of subunit 1 (except for those with asterisks) are shown.

E·PLP and E·PLP=L-MeAsp (*6*). The α- and γ-carboxylate groups interact with the guanidinium groups of Arg386 and Arg292*, respectively, in the same way as the α- and β-carboxylate and guanidinium groups of E·PLP=L-MeAsp (*6*). In comparison with E·PLP, Cα of Arg386 of E·PPx-L-MeGlu shifts by 0.65 Å (subunit 1) and 0.77 Å (subunit 2), and the guanidinium group of the side chain shifts by 0.76 Å (subunit 1) and 0.95 Å (subunit 2) toward the active site. The corresponding values for the pair of E·PLP and E·PLP=L-MeAsp are 0.80 and 0.84 Å, respectively. As a result, the guanidinium group of Arg386 forms a stable hydrogen bond/salt bridge with the α-carboxylate group of the L-MeGlu moiety.

The carboxylate groups of the ligand and the guanidinium groups of Arg292* and Arg386 are superimposable between E·PPx-L-MeGlu and E·PLP=L-MeAsp. Accordingly, the carbon chain (C3) flanked by the two carboxylate groups of L-MeGlu is more bulged compared to that (C2) of L-MeAsp. The Cβ atom of L-MeGlu is closer to the hydroxyphenyl group of Tyr70* by 1.1 Å compared to that of L-MeAsp, and van der Waals contact is expected between the L-MeGlu Cβ and Tyr70*. The torsion angle of C(carboxylate)−Cα−Cβ−Cγ is −21° (subunit 1) and −22° (subunit 2), which are the values of energetically unfavorable conformations. Therefore, a significant strain is considered to exist at the L-MeGlu moiety compared to the L-MeAsp moiety in E·PLP=L-MeAsp.

The residues Ile37-Gly38-Val39, which form a part of the "hydrophobic patch" at the entrance of the active site (*4*),

of E·PPx-L-MeGlu and E·PLP=L-MeAsp showed the same conformational change from E·PLP. The peptide bond between Ile37 and Gly38 rotates by 120°, and the side chain of Ile37 covers the active site (Figure 5A). The side-chain conformation of Ile37 and those of Leu17-Ile18, which are positioned in front of the ligand, have essentially the same conformation between the two complexes.

The Pair of E·PPx-L-MeGlu and E·PPx-D-Glu Suggests the Ketimine Structure. The crystal structure of E·PPx-D-Glu was successfully obtained and is shown in Figure 5B with the structure of E·PPx-L-MeGlu overlaid at the large domain main-chain atoms. This is the only structure of AspAT complexed with a ligand containing the D-isomer of amino acid. The carboxylate groups of the ligand, the guanidinium groups of Arg292* and Arg386, and the residues surrounding the ligand of the two complex structures are strikingly superimposable. The only difference is the position of Cα, which is 1.66 Å apart from that of E·PPx-L-MeGlu and reflects the inversed configuration of this atom between the two structures. If we convert the hybridization of this atom from sp³ to sp², we obtain the structure of the ketimine intermediate. Therefore, we can expect that the ketimine structure is a hybrid between the two overlaid structures shown in Figure 5. Interestingly, the torsion angle of C(carboxylate)−Cα−Cβ−Cγ of the D-glutamate moiety is −81° (subunit 1) and −74° (subunit 2), which are the values of energetically more favorable conformations (close to gauche) than those (close to syn) of the L-MeGlu moiety in E·PPx-L-MeGlu. Therefore, the conformation of the
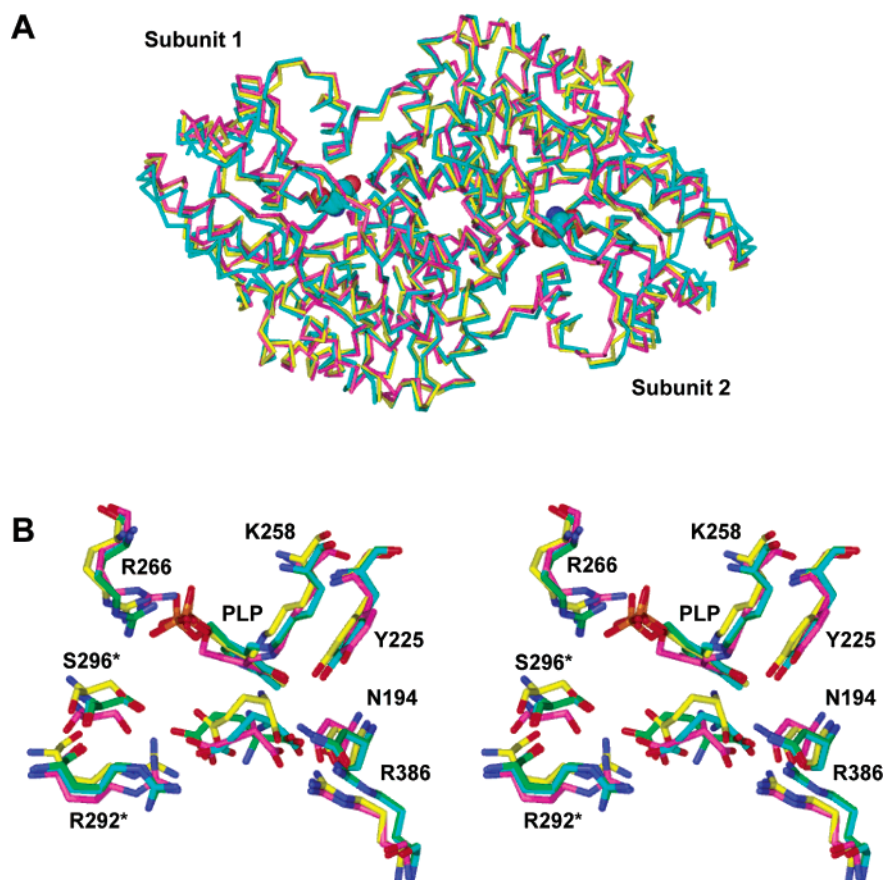
FIGURE 6: (A) Superimposed Cα traces of the energy-minimized model structures of the Michaelis complexes of AspAT with L-aspartate (E·PLP·L-Asp, magenta) and L-glutamate (E·PLP·L-Glu, cyan), together with the starting model (yellow) of E·PLP·L-glutamate built on the crystal structure of E·PPx-L-MeGlu. The bound L-glutamate of the energy-minimized structure is shown in van der Waals spheres. (B) Superimposed structures of the active site of subunit 1. The structures are distinguished by the color of the carbon atoms. The colors correspond to those used in panel A, except that the structure with carbon atoms in green is another energy-minimized structure of E·PLP·L-Glu obtained by a stochastic conformational search on the bound L-glutamate.

ketimine intermediate is expected to be energetically more favorable compared to that of E·PPx-L-MeGlu, the model for the external aldimine.

L-Glutamate Modeled in the Closed Form of AspAT Induces Conformational Change to the Open Form. L-Glutamate was modeled into the closed form of AspAT, using the crystal structure of E·PPx-L-MeGlu (Figure 6A,B, yellow). After energy minimization, C(carboxylate)−Cα−Cβ−Cγ of L-glutamate adopts a more relaxed gauche conformation (Figure 6B, cyan), the torsion angles being −62° (subunit 1) and −61° (subunit 2). As a result, the α-carboxylate group pushes the guanidinium group of Arg386, the small domain residue, to move outward of the active site. This is reflected in the overall structure (Figure 5A, cyan); the small domain is displaced to open the active site, resulting in the conformation which resembles that of the open form of E·PLP (Figure 4, cyan). The distance between the PLP−Lys258 aldimine N and the α-amino N of L-glutamate is 5.2 Å. Because the energy minimization procedure used here may result in an energetically metastable structure, a stochastic conformational search involving the dihedral angles of the L-glutamate bound to subunit 1 was performed. The atoms of the protein were again allowed to move. A structure which is 9.3 kJ mol^{-1} more stable than the "cyan" structure in Figure 6A,B was obtained and is shown with carbon atoms in green in Figure 6B. The overall

protein structure was essentially identical to that of the cyan structure (data not shown). This indicates that the cyan structure is an energetically metastable state, and there is an energy barrier between the two states (cyan and green). In the green structure (Figure 6B), C(carboxylate)−Cα−Cβ−Cγ of L-glutamate assumes a nearly anti conformation (torsion angle = −173°) and the α-amino group is opposite to the PLP−Lys258 aldimine, the distance between the two N atoms being 6.6 Å. This conformation resembles that of L-glutamate modeled in the open form of E·PLP (Figure 3B, cyan), although the hydrogen-bonding pattern involving the γ-carboxylate of L-glutamate, Arg292*, and Ser296* is slightly different between the two structures.

Energy minimization of the Michaelis complex with L-aspartate resulted in a structure (Figure 6A,B, magenta) essentially similar to that of the closed conformation of the enzyme (Figure 6A,B, yellow; this structure is that of E·PPx-L-MeGlu, but is almost completely identical to that of E·PLP=L-MeAsp as is shown in Figure 4), the distance between the α-amino N of L-aspartate and the PLP−Lys258 aldimine N being 3.7 Å. Thus, when energy minimization is carried out with all the atoms allowed to move, L-aspartate does not induce a conformational change of the closed form of E·PLP, whereas L-glutamate induces a conformational change of E·PLP from the closed to the open form.

DISCUSSION

Michaelis Complex of AspAT with C4-Dicarboxylic Acids. Before discussing the Michaelis complex of AspAT with C5 ligands, we summarize here what is known about the Michaelis complex of AspAT with C4 ligands.

The characteristic point in the Michaelis complex structure of E·PLP with a C4 amino acid is that it is an equilibrium mixture of E_L·SH^+ and $E_L H^+$·S (Scheme 1) and that there is no apparent presence of the species E_L·S and $E_L H^+$·SH^+. That is, a proton is shared by the two groups, and the two groups are never protonated or unprotonated simultaneously. This is shown by the absorption spectra of the Michaelis complex and the external aldimine complex formed by association of L-MeAsp with E·PLP. The spectra showed a pH-independent partial protonation structure, ∼7% for the Michaelis complex and ∼35% for the external aldimine (*10*).

The rationale that explains this partial protonation is shown in Figure 3A, which is a modeled structure of the Michaelis complex of E·PLP with L-aspartate based on the structure of E·PLP complexed with maleate (*4*). The α-amino group of aspartate is pointed toward the imino group of the PLP−Lys258 Schiff base (3.4 Å between the two N atoms), and there is a strong electrostatic interaction between the two groups. Therefore, in order to avoid electrostatic repulsion, only one proton must be shared by the two groups.

Michaelis Complex of AspAT with C5-Dicarboxylic Acids. During the analysis of the reaction of E·PLP with L-glutamate, we found that incorporation of the species $E_L H^+$·SH^+ was necessary to explain the pH and concentration dependency of the apparent rate constant for the decrease in absorbance at 430 nm, which represents $E_L H^+$ (*12*). The pH-dependent spectral change of the Michaelis complex of AspAT with the C5 substrate analogue, L-MeGlu, is best analyzed by the two-step dissociation model (Figure 2). Assuming that the complex of E·PLP with L-MeGlu represents the Michaelis complex with L-glutamate, the present results show that the Michaelis complex contains 4 possible combinations of the protonation structures, $E_L H^+$·SH^+, E_L·SH^+, $E_L H^+$·S, and E_L·S (Scheme 2). This indicates that the electrostatic interaction between the aldimine N and the α-amino N in the Michaelis complex with L-glutamate is much weaker than that with L-aspartate.

The proposed structure of the Michaelis complex with L-glutamate (Figure 3B) is consistent with this weak electrostatic interaction. The α-amino group of L-glutamate is pointed in the direction opposite to the imino group of the Schiff base, and the distance between the aldimine N and the α-amino N is 7.3 Å (protonated α-amino group) and 6.7 Å (unprotonated α-amino group). The model study also showed that the structure of the open form of the enzyme bound with the extended conformation of L-glutamate is energetically more stable than that of the closed form of the enzyme with the folded conformation of L-glutamate (Figure 6A,B). From these findings, we can conclude that the structure shown in Figure 4B is the most probable structure of the Michaelis complex with L-glutamate that can explain all the spectroscopic and previous kinetic data of the interaction of AspAT with C5 ligands.

Conformational Change in AspAT during the Trans-aldimination Reaction from the Michaelis Complex to the External Aldimine. Although the data presented above strongly suggest that the Michaelis complex with L-glutamate is in the open conformation, the structure of the external aldimine complex with L-glutamate is another issue to be solved. The crystal structures of E·PPx-L-MeGlu (Figures 4, 5) and E·PPx-L-Glu are in the closed form. This indicates that, once a bond is formed between the α-amino group of L-glutamate and PLP, the enzyme−C5-dicarboxylic acid complex assumes the closed conformation.

The conformational transition from the open form in the Michaelis complex to the closed form in the external aldimine is schematically explained in Figure 7. The complex of E·PLP with L-aspartate is in the closed form for both the Michaelis complex and the external aldimine (Figure 7, upper panels). The external aldimine of E·PLP with L-glutamate is also in the closed form (Figure 7, lower right). However, this structure is realized by "hooking" the α-amino group of L-glutamate to the aldehyde group of PLP, thereby placing the α-carboxylate group in the same position occupied by the α-carboxylate group of L-aspartate in the complexes of E·PLP with C4-dicarboxylic acids. The resultant structure of L-glutamate assumes an unfavorable syn conformation at C(carboxylate)−Cα−Cβ−Cγ and stores strain energy in this region. Therefore, if the bond between the α-amino N and C4′ of PLP is broken to form the Michaelis complex, L-glutamate releases its strain energy to assume an extended conformation, pushing Arg386 outward of the active site (Figure 7, lower left). This process is exactly described by the model study shown in Figure 6B. The conformational change of C(carboxylate)−Cα−Cβ−Cγ of L-glutamate from the syn conformation (yellow) to the gauche (cyan) conformation causes opening of the domain interface. This open structure of the complex is expected to be further stabilized by a conformational change of C(carboxylate)−Cα−Cβ−Cγ from gauche to anti. This strain in L-glutamate explains why AspAT assumes the open conformation in the Michaelis complex, in which the bond between the α-amino group of glutamate and PLP is not formed.

The equilibrium between the Michaelis complex and the external aldimine is difficult to evaluate. However, the following discussion is consistent with the idea that the equilibrium is shifted toward the Michaelis complex. The structure of E·PPx-L-MeGlu can be used as a model for the external aldimine complex of E·PLP with L-MeGlu or L-glutamate. The distance between the α-amino N of the L-amino acid moiety and the ε-amino group of Lys258 is 4.2 Å for E·PLP=L-MeAsp and 4.4 Å for E·PPx-L-MeGlu (Figure 5A). The spatial alignment of the residues and atoms around the ligand is essentially the same between E·PLP=L-MeAsp and E·PPx-L-MeGlu (Figure 5A). Therefore, in the external aldimine complex of E·PLP and L-MeGlu, the electrostatic interaction between the imine N of the PLP−L-MeGlu aldimine and the ε-amino group of Lys258 is considered to be strong like that of the PLP−L-MeAsp aldimine in E·PLP=L-MeAsp, and pH-independent partial protonation of the imine N is expected for the PLP−L-MeGlu aldimine. If this is the case, the strong pH dependency of the spectrum of the complex of E·PLP with L-MeGlu (Figure 2) indicates that the Michaelis complex constitutes a large part of the complex of E·PLP with L-MeGlu. Furthermore, because the PLP−L-MeAsp aldimine of E·PLP=L-MeAsp is ∼35% protonated (*10*), if we assume that the protonation status of the PLP−L-MeGlu aldimine is similar to that of
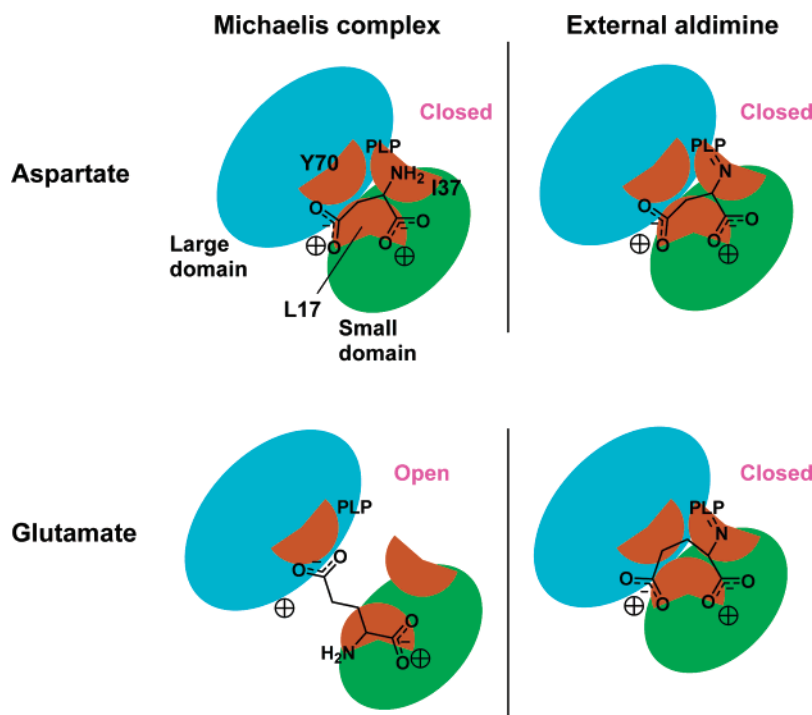
FIGURE 7: Schematic description of the recognition mechanism of C5 subtrates in comparison to C4 substrates. Hydrophobic residues are shown in half-balls.

the PLP−L-MeAsp aldimine, the low value of the 430 nm absorption at high pH (Figure 2) indicates that the external aldimine complex constitutes only a minor part of the complex of E·PLP with L-MeGlu. Thus, the equilibrium between the Michaelis complex and the external aldimine is shifted toward the Michaelis complex. This is apparently caused by the strain energy of the puckered conformation of the PLP−L-MeGlu external aldimine.

Driving Force That Promotes Transition to the Closed Form. As a consequence of the above discussion, there must be a driving force from the Michaelis complex to the external aldimine, in order to drive the catalytic reaction of AspAT with L-glutamate effectively. Free energies that are released on formation of the external aldimine from the Michaelis complex can be such a driving force. In the case of the reaction with L-glutamate, this step involves the conformational change in AspAT. In this respect, the residues at the entrance of the active site, i.e., the "hydrophobic patch" residues (*3*, *4*), are highlighted.

Among the "hydrophobic patch" residues, Tyr70* is located in the large domain, whereas Ile18 and Val39 are in the small domain. These hydrophobic residues interdigitate with each other in the closed conformation. In addition, a van der Waals interaction between Cβ of the C5 ligand and the hydroxyphenyl group of Tyr70* is expected to be present in the external aldimine but not in the Michaelis complex (see Results; Figures 3B and 5A). Thus, the hydrophobic interaction between these residues will contribute to shift the equilibrium from the Michaelis complex to the external aldimine. In this respect, the finding that Tyr70 is important for the recognition of L-glutamate (*23*) is of interest. Mutation of Tyr70* to Phe, which keeps the hydrophobic interaction as described above, has a similar effect on the k_{cat} values with C4 and C5 substrates. On the other hand, mutation to Ser has a more deteriorating effect on the k_{cat} values with

C5 substrates than those with C4 substrates. This can be explained by assuming that the phenyl ring of Tyr70* is involved in the interaction of Tyr70* with the side chains of Val39 and Ile18 and with the C5 ligand to promote the transition from the Michaelis complex to the external aldimine, showing the importance of the phenyl ring in the catalytic step of the reaction with the C5 substrates.

Finally, the set of the crystal structures of E·PPx-L-MeGlu and E·PPx-D-Glu strongly suggests that the ketimine complex of E·PMP with 2-oxoglutarate will assume an intermediate structure of these two structures. That is, the ketimine complex in the C5 reaction is expected to be in the closed form, and this is in agreement with the crystallographic study by Malashkevich, Toney, and Jansonius (*24*), in which L-glutamate was substituted with the bound maleate in the E·PLP·maleate crystal. Because the glutarate complex of E·PMP is in the open form (*7*), it is concluded that, for the C5 reaction of AspAT (eq 2), the enzyme is in the closed form from the external aldimine to the ketimine and that both the Michaelis complexes with L-glutamate and 2-oxoglutarate are in the open form.

REFERENCES

1. Kiick, D. M., and Cook, P. F. (1983) pH studies toward the elucidation of the auxiliary catalyst for pig heart aspartate aminotransferase, *Biochemistry 22*, 375−382.
2. Jansonius, J. N., and Vincent, M. G. (1987) Structural basis for catalysis by aspartate aminotransferase, in *Biological Macromolecules and Assemblies* (Jurnak, F. A., McPherson, A., Eds.) Vol. 3, pp 187−285, Wiley and Sons, New York.
3. McPhalen, C. A., Vincent, M. G., Picot, D., Jansonius, J. N., Lesk, A. M., and Chothia, C. (1992) Domain closure in mitochondrial aspartate aminotransferase, *J. Mol. Biol. 227*, 197−213.
4. Jäger, J., Moser, M., Sauder, U., and Jansonius, J. N. (1994) Crystal structures of *Escherichia coli* aspartate aminotransferase in two conformations. Comparison of an unliganded open and two liganded closed forms, *J. Mol. Biol. 239*, 285−305.

5. Rhee, S., Silva, M. M., Hyde, C. C., Rogers, P. H., Metzler, C. M., Metzler, D., E., and Arnone, A. (1997) Refinement and comparisons of the crystal structures of pig cytosolic aspartate aminotransferase and its complex with 2-methylaspartate, *J. Biol. Chem. 272*, 17293−17302.

6. Okamoto, A., Higuchi, T., Hirotsu, K., Kuramitsu, S., and Kagamiyama, H. (1994) X-ray crystallographic study of pyridoxal 5′-phosphate-type aspartate aminotransferases from *Escherichia coli* in open and closed form, *J. Biochem. 116*, 95−107.

7. Miyahara, I., Hirotsu, K., Hayashi, H., and Kagamiyama, H. (1994) X-ray crystallographic study of pyridoxamine 5′-phosphate-type aspartate aminotransferases from *Escherichia coli* in three forms, *J. Biochem. 116*, 1001−1012.

8. Malashkevich, V. N., Onuffer, J. J., Kirsch, J. F., and Jansonius, J. N. (1995) Alternating arginine-modulated substrate specificity in an engineered tyrosine aminotransferase, *Nat. Struct. Biol. 2*, 548−553.

9. Toney, M. D., and Kirsch, J. F. (1993) Lysine 258 in aspartate aminotransferase: enforcer of the Circe effect for amino acid substrates and general-base catalyst for the 1,3-prototropic shift, *Biochemistry 32*, 1471−1479.

10. Hayashi, H., Mizuguchi, H., and Kagamiyama, H. (1998) The imine-pyridine torsion of the pyridoxal 5′-phosphate Schiff base of aspartate aminotransferase lowers its pK_a in the unliganded enzyme and is crucial for the successive increase in the pK_a during catalysis, *Biochemistry 37*, 15076−15085.

11. Ovchinnikov, Y. A., Egorov, C. A., Aldanova, N. A., Feigina, M. Y., Lipkin, V. M., Abdulaev, N. G., Grishin, E. V., Kiselev, A. P., Modyanov, N. N., Braunstein, A. E., Polyanovsky, O. L., and Nosikov, V. V. (1973) The complete amino acid sequence of cytoplasmic aspartate aminotransferase from pig heart, *FEBS Lett. 29*, 31−34.

12. Islam, M. M., Hayashi, H., and Kagamiyama, H. (2003) Reaction of aspartate aminotransferase with C5-dicarboxylic acids: comparison with the reaction with C4-dicarboxylic acids, *J. Biochem. 134*, 277−285.

13. Inoue, Y., Kuramitsu, S., Inoue, K., Kagamiyama, H., Hiromi, K., Tanase, S., and Morino, Y. (1989) Substitution of a lysyl residue for arginine 386 of *Escherichia coli* aspartate aminotransferase, *J. Biol. Chem. 264*, 9673−9681.

14. Jancarik, J., and Kim, S. H. (1991) Sparse matrix sampling: a screening method for crystallization of proteins, *J. Appl. Crystallogr. 24*, 409−411.

15. Collaborative Computational Project Number 4 (1994) *Acta Crystallogr., Sect. D 50*, 760−763.

16. Jones, T. A., Zou, J. Y., Cowan, S. W., and Kjeldgaard, M. (1991) Improved methods for building protein models in electron density maps and the location of errors in these models, *Acta Crystallogr. A47*, 110−119.

17. Brünger, A. T., Adams, P. D., Clore, G. M., DeLano, W. N., Gross, P., Grosse-Kunstleve, R. W., Jiang, J.-S., Kuszeski, J., Nilges, M., Pannu, N. S., Read, R. J., Rice, L. M., Simonson, T., and Warren, G. L. (1998) Crystallography & NMR system: A new software suite for macromolecular structure determination, *Acta Crystallogr., Sect. D 54*, 905−921.

18. Laskowski, R. A., MacArthur, M. W., Moss, D. S., and Thornton, J. M. (1993) PROCHECK: a program to check the stereochemical quality of protein structures, *J. Appl. Crystallogr. 26*, 283−291.

19. Schnackerz, K. D. (1984) Phosphorus-31 nuclear magnetic resonance study on cytoplasmic aspartate aminotransferase from pig heart. A reinvestigation, *Biochim. Biophys. Acta 789*, 241−244.

20. Koradi, R., Billeter, M., and Wuthrich, K. (1996) MOLMOL: a program for display and analysis of macromolecular structures, *J. Mol. Graphics 14*, 51−55.

21. DeLano, W. L. (2002) The PyMOL User's Manual, DeLano Scientific, San Carlos, CA.

22. Fasella, P., Giartosio, A., and Hammes, G. G. (1966) The interaction of aspartate aminotransferase with alpha-methylaspartic acid, *Biochemistry 5*, 197−202.

23. Inoue, K., Kuramitsu, S., Okamoto, A., Hirotsu, K., Higuchi, T., and Kagamiyama, H. (1991) Site-directed mutagenesis of *Escherichia coli* aspartate aminotransferase: role of Tyr70 in the catalytic processes, *Biochemistry 30*, 7796−7801.

24. Malashkvich, V. N., Toney, M. D., and Jansonius, J. N. (1993) Crystal structures of true enzymatic reaction intermediates: aspartate and glutamate ketimines in aspartate aminotransferase, *Biochemistry 32*, 13451−13462.